JOURNAL OF
biomaterials
applications

Journal of Biomaterials Applications
2014, Vol. 29(5) 639–653

DOI: 10.1177/0885328214539824
jba.sagepub.com
SAGE

Effect of boron oxide addition on fibre drawing, mechanical properties and dissolution behaviour of phosphate-based glass fibres with fixed 40, 45 and 50 mol% P_2O_5

Nusrat Sharmin, Andrew J Parsons, Chris D Rudd and Ifty Ahmed

Abstract

Previous studies investigating manufacture of phosphate-based glass fibres from glasses fixed with P_2O_5 content less than 50 mol% showed that continuous manufacture without breakage was very difficult. In this study, nine phosphate-based glass formulations from the system P_2O_5-CaO-Na_2O-MgO-B_2O_3 were prepared with P_2O_5 contents fixed at 40, 45 and 50 mol%, where Na_2O was replaced by 5 and 10 mol% B_2O_3 and MgO and CaO were fixed to 24 and 16 mol%, respectively. The effect of B_2O_3 addition on the fibre drawing, fibre mechanical properties and dissolution behaviour was investigated. It was found that addition of 5 and 10 mol% B_2O_3 enabled successful drawing of continuous fibres from glasses with phosphate (P_2O_5) contents fixed at 40, 45 and 50 mol%. The mechanical properties of the fibres were found to significantly increase with increasing B_2O_3 content. The highest tensile strength (1200 ± 130 MPa) was recorded for $45P_2O_5$-$16CaO$-$5Na_2O$-$24MgO$-$10B_2O_3$ glass fibres. The fibres were annealed, and a comparison of the mechanical properties and mode of degradation of annealed and non-annealed fibres were investigated. A decrease in tensile strength and an increase in tensile modulus were observed for the annealed fibres. An assessment of the change in mechanical properties of both the annealed and non-annealed fibres was performed in phosphate-buffered saline (PBS) at 37°C for 28 and 60 days, respectively. Initial loss of mechanical properties due to annealing was found to be recovered with degradation. The B_2O_3-containing glass fibres were found to degrade at a much slower rate as compared to the non-B_2O_3-containing fibres. Both annealed and non-annealed fibres exhibited a peeling effect of the fibre's outer layer during degradation.

Keywords

Phosphate glass fibres, fibre drawing, mechanical properties, annealing, dissolution behaviour

Introduction

Phosphate-based glasses (PBGs) are unique materials as they can resorb completely in aqueous media, and their resorption rates can easily be altered via the addition of different modifier oxides. PBGs are completely amorphous and have been drawn into fibres from varying formulations.[1–3] In addition, the chemical composition of PBGs can be made to closely resemble that of natural bone.[4] The properties of PBGs have been of special interest for the development of bioresorbable materials as temporary implants or in tissue-engineering[2] applications. The structure of PBGs is composed of an inorganic phosphate network in which PO_4^{3-} tetrahedral units are the main building blocks. The presence of modifying oxides disrupts the glass structure replacing bridging oxygen with non-bridging oxygen. The structure of the PBGs can be varied from a cross-linked network of tetrahedra in vitreous P_2O_5 (Q^3 units) to polymer-like chains of tetrahedra in

Division of Materials, Mechanics and Structures, University of Nottingham, Nottingham, UK

Corresponding author:
Ifty Ahmed, Division of Materials Mechanics and Structures (MMS), University Park Campus, University of Nottingham, Nottingham NG7 2RD, UK.
Email: ifty.ahmed@nottingham.ac.uk

meta phosphate glasses (Q^2 units) to invert glasses based on small pyro- (Q^1 units) and orthophosphate (Q^0 units) anions, depending on the type and amount of modifying oxides that are added.[5]

For a number of years now, phosphate-based glass fibres (PGF) have been evaluated as a material for varying tissue-engineering applications, especially for tissue with a medium to high anisotropy such as muscle due to their combination of suitable chemistry and morphology, which can mimic the fibrous nature of these tissues.[2,6,7] The mechanical strength and elastic properties of the fibres are very different from the glass with the same composition, which have enabled a broad field of application for these fibres.[8] These PGFs have high-mechanical properties (tensile strength ~318–484 MPa and tensile modulus ~50–75 GPa), and a number of studies have shown that the PGFs have great potential to be used as reinforcement materials in biodegradable composites for applications such as bone fracture-fixation devices.[9,10]

PGFs are fabricated conventionally via a melt-drawn system where fibres are drawn from a high-temperature glass melt and collected on a rotating drum. Ahmed et al.[1] worked with a range of PBGs in the system P_2O_5-CaO-Na_2O with P_2O_5 content fixed to 45, 50 and 55 mol% and were able to draw fibres from glasses with fixed 50 and 55 mol% P_2O_5. However, they found that manufacturing fibres from glasses with fixed 45 mol% P_2O_5 proved to be extremely difficult, which was suggested to be due to the structure of these glasses. They conducted NMR analysis, which revealed that both Q^1 and Q^2 species were present in glasses with fixed 45 mol% P_2O_5, whilst only Q^2 species were found with fixed 50 and 55 mol% P_2O_5 compositions.[4] They concluded that the chain length in the glasses played a very important role in the fibre-drawing process, and glasses with Q^2 structure (i.e. infinite chain length) were easier to draw into fibre form than glasses composed of shorter chain lengths (i.e. with Q^1s).

Recently, PGF-reinforced composites have been investigated as potential bone fracture-fixation devices due to their mechanical properties and also due to the similarity between the chemical compositions of the reinforcing fibres with the inorganic component of natural bone.[11,12] The flexural strength and modulus of PGF/PLA composites with varying fibre formulations, fibre volume fraction and fibre alignment have been reported to be in the range of 80–300 MPa and 5–25 GPa, respectively.[9,12,13] Controlled degradation rates play a very important role in the field of resorbable materials for bone regeneration.[14] In this respect, PGF offers a distinct advantage over other materials as their degradation rate can be controlled just by changing the composition to suit the end application.

Borophosphate glasses have been the topic of study for their variety of established and novel applications including fast ion conductors, sealing glasses and solder glasses.[15–18] It is worth noting that both the boron and phosphorus are network formers, and a wide variety of glass network structures can be expected from the combination of these two glass network formers.[17,19] NMR analysis of borophosphate glasses in the system of $CaO–B_2O_3–P_2O_5$ revealed that the addition of boron increased the chain lengths (Q^2 species) in the glass structure.[16] Several studies also showed that addition of B_2O_3 to the phosphate network improved the chemical durability and thermal properties of the glasses.[20–23] In addition, B_2O_3 is known to improve the thermal stability of PBGs by suppressing their tendency to crystallise,[22,24] which is a common problem associated with the drawing of PBG fibres as they have a tendency towards crystallisation at the working process temperature,[25] particularly with Q^0 and Q^1-dominated structures. Therefore, it was hypothesised in our current study that addition of boron may overcome this problem and make the fibre-drawing process easier and continuous; especially for glasses with phosphate contents lower than 50 mol%.

Therefore, this study aimed to investigate the effect of B_2O_3 addition on the feasibility of the fibre-drawing process for the following glass systems: $(P_2O_5)_{40}$-$(CaO)_{16}$-$(Na_2O)_{20-x}$-$(MgO)_{24}$-$(B_2O_3)_x$, $(P_2O_5)_{45}$-$(CaO)_{16}$-$(Na_2O)_{15-x}$-$(MgO)_{24}$-$(B_2O_3)_x$ and $(P_2O_5)_{50}$-$(CaO)_{16}$-$(Na_2O)_{10-x}$-$(MgO)_{24}$-$(B_2O_3)_x$, where $x = 0$, 5 and 10 mol%. The initial and main challenge of our study was to produce glass formulations with less than 50 mol% P_2O_5, which could be drawn into continuous fibres from the melt. The main reason for attempting to achieve this was that previous studies from the group had shown a much more favourable cytocompatible response for PBG formulations with less than 50 mol% P_2O_5, however, proved very difficult to fiberise. The results from this study showed that continuous fibres from PBG formulations with P_2O_5 contents of 40 and 45 mol% could be fiberised continuously without breaking with addition of B_2O_3.

In addition, we also wanted to evaluate the effect of B_2O_3 addition on the mechanical properties of the as drawn and annealed fibres. A dissolution study of as drawn and annealed fibres was also carried out in PBS for 2 months at 37°C in order to investigate any changes in their mechanical properties during degradation.

Materials and methods

Phosphate glass production

Nine glass compositions were prepared using the following precursors: sodium dihydrogen phosphate

Table 1. Glass codes, drying and melting temperature used throughout the study.

Glass code	P_2O_5 content (mol%)	CaO content (mol%)	Na_2O content (mol%)	MgO content (mol%)	B_2O_3 content (mol%)	Dry temp/time (°C/h)	Melt temp/time (°C/h)
P40 B0	40	16	20	24	–	350/1	1150/1.5
P40 B5	40	16	15	24	5	350/1	1150/1.5
P40 B10	40	16	10	24	10	350/1	1150/1.5
P45 B0	45	16	15	24	–	350/1	1150/1.5
P45 B5	45	16	10	24	5	350/1	1150/1.5
P45 B10	45	16	5	24	10	350/1	1150/1.5
P50 B0	50	16	10	24	–	350/1	1150/1.5
P50 B5	50	16	5	24	5	350/1	1150/1.5
P50 B10	50	16	–	24	10	350/1	1150/1.5

(NaH_2PO_4), calcium hydrogen phosphate ($CaHPO_4$), magnesium hydrogen phosphate trihydrate ($MgHPO_4.3H_2O$), boron oxide (B_2O_3) and phosphorus pentoxide (P_2O_5) (Sigma Aldrich, UK) as starting materials. The precursors were mixed together and transferred to a 100-ml volume Pt/5% Au crucible (Birmingham Metal Company, UK), which was then placed in a furnace (which had been preheated to 350°C) for half an hour for the removal of H_2O. The salt mixtures were then melted in a furnace at 1150°C for 1.5 h, depending on the glass composition as shown in Table 1. The resulting molten glass was poured onto a steel plate and left to cool to room temperature. The glass was then kept in a desiccator until further use.

Fibre-drawing process

Continuous fibres approximately ~20 µm diameter were produced via a melt-draw spinning process using a dedicated in-house facility. The pulling temperature was adjusted to around 1150°C. The fibres were annealed for 60 min at 10°C above the glass transition temperature prior to use. The heating cycle involved a 20°C min^{-1} ramp to 200°C, followed by 5°C min^{-1} to $T_g + 10$°C, 60-min dwell, cooling to 20°C at 5°C min^{-1}.

Dissolution of fibres

A dissolution study was conducted on both the annealed and non-annealed glass fibres. The fibres were cut into an average length of 50 mm, and approximately 300 mg of each fibre type was placed into individual glass vials, each containing 30 ml of PBS solution. The time points used for annealed fibres were days 1, 7, 14, 21, 28, 35, 45 and 60. The time points for non-annealed fibres were days 1, 7, 14, 21 and 28. At each time point, the pH of the solution was measured using a microprocessor pH meter (Hanna, UK). The pH electrode was calibrated using standard pH buffer solutions at pH 4.0 and pH 7.0 (Fisher Scientific, UK) prior to each measurement. The PBS solution was changed at each time point. After degradation, the PBS solution was removed from the fibre (taking care to avoid loss of any fibres with the media), and the fibres were then dried in a drying oven at 50°C for 24 h.

Helium pycnometry

The density of the fibres was determined by using a Micromeritics AccuPyc 1330 helium pycnometer (Norcross, GA, USA). The equipment was calibrated using a standard calibration ball (3.18551 cm^3) with errors of ±0.05%. The fibres, with an average weight of approximately 1.0 g, were used for the density measurements, and the process was repeated three times.

Single fibre filament test

Single fibre filament tests (SFTT) were conducted in accordance with ISO 11566.[26] Twenty fibres were mounted individually onto plastic tabs for each sample, with a 25-mm gauge length testing setup. The ends of each fibre were bonded to the plastic tab with an acrylic adhesive (Dymax 3099-Dymax, Europe), and the adhesive was cured using UV light. In order to determine the individual diameter of each fibre prior to testing, the fibre specimens were measured by using a laser scan micrometer, LSM 6200 (Mitutoyo, Japan). The laser scan micrometer was calibrated with glass fibre of known diameters (determined by SEM), and the error on diameter measurements is considered to be ±0.3 µm. The SFTT was performed using a LEX810 Tensile Tester (UK) at room temperature with a load capacity of 0.2 N and a speed of 0.017 mm s^{-1}. The Student's t-test was used to study

the effect of composition on the tensile strength and modulus values of the fibres. Significance was detected at a 0.05 level, and all statistical analysis was carried out using GraphPad Prism for Windows (GraphPad, Software Inc, USA).

The Weibull distribution is a well known and accepted method to describe the strength of fibres.[27] Weibull modulus and normalising stress are found statistically as the shape and scale factors. The normalising stress σ_o can be regarded as the most probable stress at which a fibre of length L_o will fail. PBG fibres are essentially brittle, and Weibull distribution is an accepted statistical tool used to characterise the failure mode of brittle fibres. In this study, Weibull parameters were obtained from the tensile strength data calculated using Minitab® 15 (version 3.2.1).

SEM analysis

Scanning electron microscope images were taken to examine the change in surface morphology of the annealed and non-annealed fibres as they degraded. The fibres were carbon coated prior to examination and viewed with a Philips XL30 scanning electron microscope operated at 20 kV.

Estimated dissolution rate of the fibres

The dissolution rate of annealed and non-annealed fibres was estimated using the change in diameter of the fibres over the time. The total surface area of the fibres was calculated using the following equation

$$\text{Surface area, A} = 2\pi r^2 + 2\pi rl$$

where r is the radius of the fibres and l the length of the fibres.

The diameter of the fibres is assumed to decrease at a similar rate for the entire fibre length. The mass of the fibres was calculated from their volume and density by using the following equation

$$\text{Mass of the fibres m} = \rho \times V$$

where ρ is the density of the fibres and V the volume of the fibres $= \pi r^2 l$.

The dissolution rate of the fibres was calculated as the average mass loss per unit area per unit time, measured at each time point.

Statistical analyses

Average values and standard deviation were computed, and statistical analysis was performed using the Prism software package (version 3.02, GraphPad Software, San Diego, California, USA, www.graphpad.com). Two-way analysis of variance was calculated with the Bonferroni post-test to compare the significance of change in one factor with time. The error bars presented represent standard deviation with $n = 20$.

Results

Mechanical properties of as-drawn non-annealed fibres

Figure 1 shows the effect of increasing P_2O_5 and B_2O_3 on the mechanical properties (tensile strength and modulus) of the fibres. An increase in tensile strength was seen with an increase in B_2O_3 content. The tensile strength of P40B0, P45B0 and P50B0 was 450 ± 76, 530 ± 67 and 649 ± 65 MPa, while the tensile strength increased to 777 ± 95, 1050 ± 141 and 983 ± 143 MPa for P40B5, P45B5 and P50B5 glass formulations, respectively. The tensile strength of P50B10 fibres is not reported as it was not possible to pull the fibres due to the high viscosity of the glass system. The highest tensile strength (1200 ± 146) MPa was observed for the P45B10 fibres. An increase in tensile strength from 450 ± 56 MPa to 649 ± 65 MPa of the P_2O_5-CaO-MgO-Na_2O glass system was also observed with increasing P_2O_5 from 40 to 50 mol%. Table 2 gives the Weibull distribution of the tensile strength of the fibres in P40, P45 and P50 glass systems, respectively. It was observed that the trend of normalising strength (σ_o) was consistent with the trend of average tensile strength. The Weibull modulus of these fibres was seen to range from 7.7 to 10.5.

The P_2O_5-CaO-MgO-Na_2O glass fibres showed a decrease in modulus from 56.5 ± 2 to $53.4 \pm 1$with increasing P_2O_5 content from 40 to 45 mol%. The difference in tensile modulus values for glass fibres with 45 and 50 mol% P_2O_5 content was not seen to be statistically significant ($P > 0.05$). Addition of 5 mol% B_2O_3 to P40, P45 and P50 glasses revealed an increase in tensile modulus to 59.2 ± 3, 59.6 ± 2 and 61.39 ± 3 GPa, respectively. However, further addition of B_2O_3 (10 mol%) did not reveal any significant improvements in the tensile modulus.

Mechanical properties of annealed fibres

A comparison of mechanical properties for annealed and non-annealed fibres was made prior to their dissolution study. Figure 2(a) and (b) showed a decrease in tensile strength and an increase in tensile modulus for annealed fibres. For non-B_2O_3-containing glass fibres, the tensile strength reduced by approximately 45% of

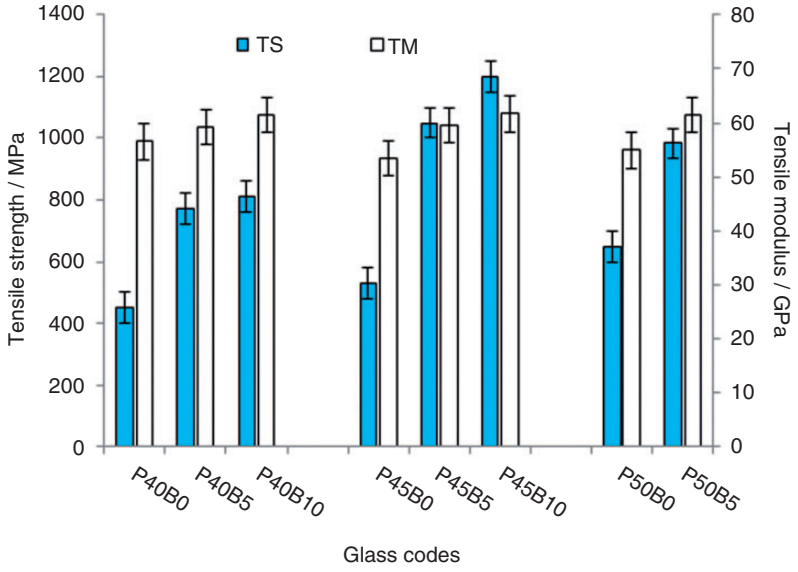

Figure 1. Tensile strength and modulus of the non-annealed fibres in the glass system P40Ca16Mg24Na(20 − X)Bx P45Ca16Mg24Na(15 − X)Bx and P50Ca16Mg24Na(10 − X)Bx (where x = 0, 5 and 10 mol%). Error bars represent the standard deviation where n = 20.

Table 2. Weibull distribution of fibres in the glass system of (a) $P_{40}Ca_{16}Mg_{24}Na_{(20-X)}B_x$, (b)$P_{45}Ca_{16}Mg_{24}Na_{(15-X)}B_x$ and (c)$P_{50}Ca_{16}Mg_{24}Na_{(10-X)}B_x$ (where x = 0, 5 and 10 mol%).

Glass codes	Tensile strength (MPa)	Normalising strength σ_o (MPa)	Weibull modulus *m*
P40B0	446.2 ± 57	475.6	7.7
P40B5	777.5 ± 96	820.9	8.1
P40B10	810.5 ± 111	855.1	9.5
P45B0	530.3 ± 67	559.1	7.9
P45B5	1050.6 ± 130	1111.0	8.1
P45B10	1200.0 ± 146	1259.0	10.2
P50B0	649.1 ± 66	679.6	10.5
P50B5	983.9 ± 143	1045.0	7.7

The tensile strength values are also included for the ease of comparison.

the original value ($P < 0.001$), whilst a reduction of around 60% in the tensile strength was observed for the B_2O_3-containing glass fibres. After annealing, the tensile modulus for P40B0, P45B0 and P50B0 fibres was seen to increase by 11, 6% and 7%, whereas as a 10, 8% and 7% reduction ($P < 0.001$) in tensile modulus was observed for P40B5, P45B5 and P50B5 fibres.

The effect of annealing on the density of the fibres was also evaluated (Figure 3). It was found that the density of the annealed fibres was significantly ($P < 0.001$) higher than the non-annealed ones.

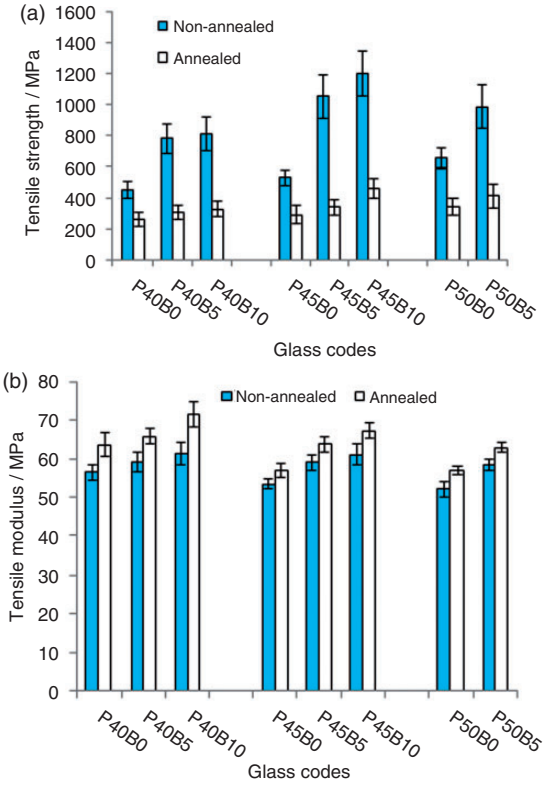

Figure 2. Tensile strength (a) and modulus (b) of annealed and non-annealed fibres in the glass system P40Ca16Mg24Na(20 − X)Bx P45Ca16Mg24Na(15 − X)Bx and P50Ca16Mg24Na(10 − X)Bx (where x = 0, 5 and 10 mol%). Error bars represent the standard deviation where n = 20.

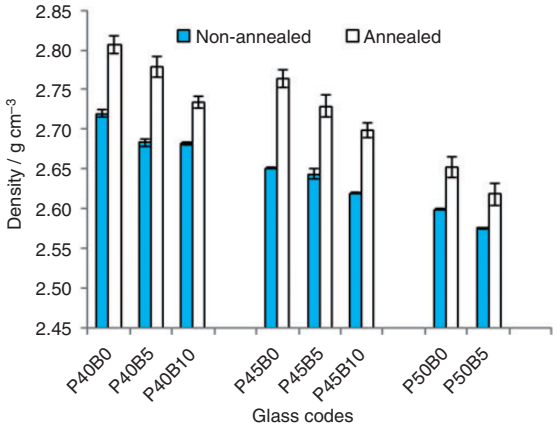

Figure 3. Effect of annealing on the density of fibres in the glass system P40Ca16Mg24Na(20 − X)Bx P45Ca16Mg24Na(15 − X)Bx and P50Ca16Mg24Na(10 − X)Bx (where x = 0, 5 and 10 mol%). Error bars represent the standard deviation where n = 20.

Mechanical properties of the annealed degraded fibres

The tensile strength for annealed and degraded P40, P45 and P50 fibres is shown in Figure 4(a) to (c), respectively. The corresponding surface morphologies of the degraded fibres via SEM are shown in Figure 5. The change in tensile modulus of the fibres with degradation is listed in Table 3. From the glass formulations investigated, it was possible to handle and test fibres from the 5 and 10 mol% B_2O_3-containing glass fibres, which had been immersed for up to 60 days. However, it was not possible to test the non-B_2O_3-containing glass fibres after 21 days of immersion in PBS as the fibres became extremely brittle and broke when handled. Also, for these non-B_2O_3-containing glass fibres, no statistically significant difference ($P > 0.05$) in tensile strength was observed up to the day-21 interval. For the B_2O_3-containing glass fibres,

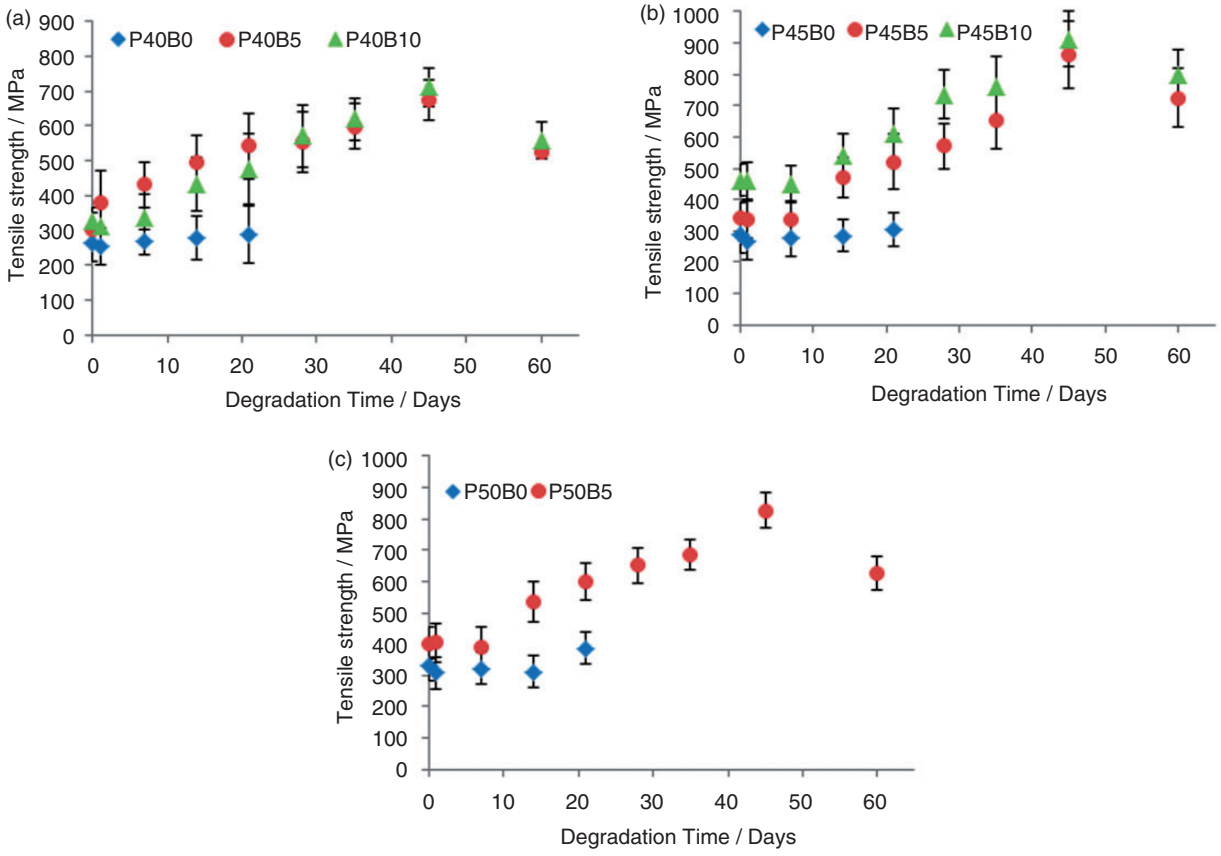

Figure 4. Change in tensile strength for annealed fibres over time in the glass system of P40Ca16Mg24Na(20 − X)Bx (a), P45Ca16Mg24Na(15 − X)Bx (b) and P50Ca16Mg24Na(10 − X)Bx (c), where x = 0, 5 and 10 mol% during degradation in PBS at 37°C. It was not possible to handle and test the P40B0, P45B0 and P50B0 fibres after 21 days of degradation. Error bars represent the standard deviation where n = 20.

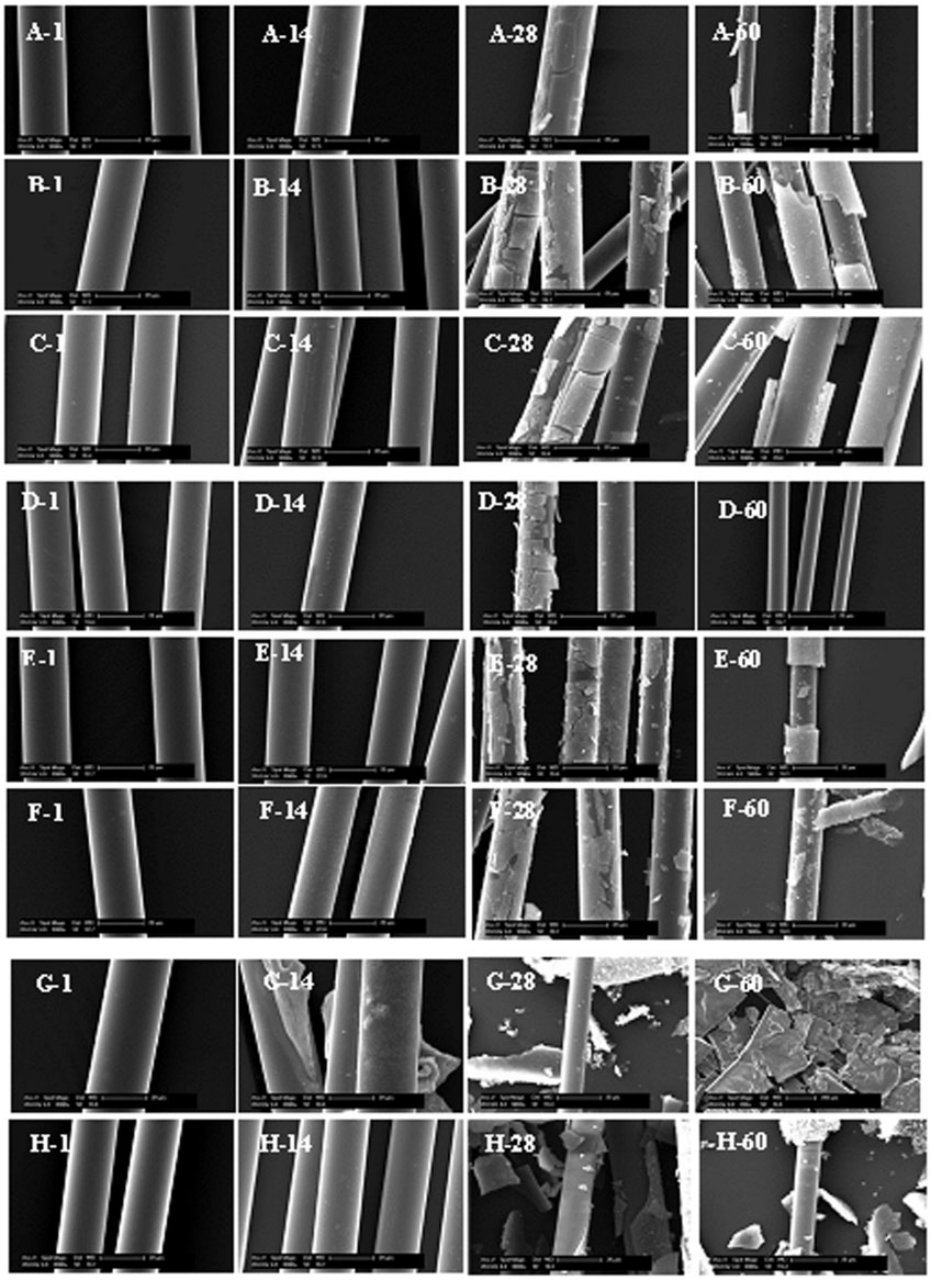

Figure 5. Scanning electron microscopy of days 1, 14, 28 and 60 annealed degraded fibres of the composition P40B0 (A1–A60), P40B5 (B1–B60), P40B10 (C1–C60), P45B0 (D1–D60), P45B5 (E1–E60), P45B10 (F1–F60), P50B0 (G1–G60) and P40B0 (H1–H60). The fibres were degraded in PBS at 37°C for up to 60 days.

no statistically significant difference ($P > 0.05$) in tensile strength was observed between day 0, 1 and 14-degraded fibres. However, the tensile strength of the day 21-degraded fibres was significantly higher ($P < 0.0001$) than the day 0 fibres. For P40B5, P45B5 and P50B5 fibres, the tensile strength of the day 14-degraded fibres was 62%, 38% and 38% higher than the day 0 fibres. However, the tensile strength for P40B10 and P45B10 at day 21 increased by 33% and 16% as compared to day 0. Further degradation of the B_2O_3-containing glass formulations revealed an increase in tensile strength values up to the day-45 interval and was then seen to decrease by the day-60 interval. However, the tensile strength of the day 60-degraded fibres was still significantly ($P < 0.05$) higher than the day 0 fibres. No statistically significant change in the fibre tensile modulus was observed over the same period of degradation (see Table 3). The corresponding

Table 3. The change in tensile modulus of the annealed and non-annealed fibres in the glass system of $P_{40}Ca_{16}Mg_{24}Na_{(20-x)}B_x$ (a), $P_{45}Ca_{16}Mg_{24}Na_{(15-x)}B_x$ (b) and $P_{50}Ca_{16}Mg_{24}Na_{(10-x)}B_x$ (c), where x = 0, 5 and 10 mol% during degradation in PBS at 37°C.

Tensile modulus of annealed fibres (GPa)

	P40B0	P40B5	P40B10	P45B0	P45B5	P45B10	P50B0	P50B10
Day 0	63.6 ± 2	65.7 ± 3	71.5 ± 3	62.1 ± 1	63.8 ± 2	67.1 ± 3	56.9 ± 2	62.9 ± 1
Day 1	61.3 ± 4	67.0 ± 6	69.6 ± 5	60.1 ± 4	65.2 ± 3	66.8 ± 4	54.2 ± 5	61.8 ± 3
Day 7	61.4 ± 4	67.1 ± 1	65.1 ± 7	58.2 ± 3	65.8 ± 4	68.2 ± 3	54.6 ± 4	61.0 ± 2
Day 14	62.1 ± 4	67.9 ± 7	65.7 ± 5	62.8 ± 6	62.9 ± 2	70.3 ± 3	55.8 ± 4	60.6 ± 4
Day 21	60.9 ± 5	68.5 ± 6	66.1 ± 4	61.4 ± 6	63.6 ± 5	68.7 ± 8	51.9 ± 3	58.5 ± 5
Day 28		72.1 ± 5	66.2 ± 7		66.5 ± 8	71.0 ± 5		62.5 ± 3
Day 35		71.5 ± 4	68.4 ± 3		71.3 ± 8	71.7 ± 4		64.8 ± 5
Day 45		69.8 ± 5	73.2 ± 5		72.7 ± 7	74.0 ± 6		69.8 ± 4
Day 60		68.5 ± 3	71.9 ± 5		71.6 ± 4	72.3 ± 5		68.2 ± 7

Tensile modulus of non-annealed fibres (GPa)

	P40B0	P40B5	P40B10	P45B0	P45B5	P45B10	P50B0	P50B5
Day 0	56.5 ± 3	59.2 ± 2	61.3 ± 3	53.4 ± 2	59.1 ± 2	61.2 ± 2	52.0 ± 1	58.3 ± 1
Day 1	54.9 ± 2	64.9 ± 3	64.2 ± 2	52.6 ± 2	63.1 ± 5	63.6 ± 2	51.3 ± 2	60.0 ± 1
Day 7	53.8 ± 1	63.5 ± 3	64.7 ± 3	52.3 ± 2	62.3 ± 4	63.0 ± 4		59.2 ± 3
Day 14		62.8 ± 4	61.5 ± 4		61.6 ± 4	57.0 ± 5		58.7 ± 2
Day 21		58.2 ± 3	58.4 ± 3		56.7 ± 4	57.5 ± 4		59.1 ± 3
Day 28		56.1 ± 4	57.2 ± 3		55.4 ± 5	55.2 ± 3		57.2 ± 3

Error bars represent the standard deviation where n = 20.

SEM images of day 1, 14, 28 and 60-degraded fibres clearly showed a decrease in diameter with degradation over time.

Mechanical properties of the non-annealed degraded fibres

The dissolution profile of the non-annealed fibres in PBS at 37°C up to the 28-day interval and the corresponding surface morphologies are shown in Figures 5 and 6. The change in tensile modulus of the fibres with degradation is listed in Table 3. These non-annealed B_2O_3-containing glass fibres could be tested up to 28-day interval of immersion, whilst it was not possible to test the non-B_2O_3-containing fibres after only 7 days of immersion as they were too brittle to handle. A peeling effect on the fibre surface was seen from day 14-degraded fibres. At the day-1 and -7 intervals, the tensile strength for these fibres was seen to decrease rapidly to almost half of their initial values. After 1-day immersion, the tensile strength for P40B5, P45B5 and P50B5 fibres had decreased from 771 ± 107, 1050 ± 165 and 983 ± 143 MPa to 286 ± 75, 308 ± 76 and 336 ± 61 MPa, respectively. With further increase in immersion time up to 28 days, a reduction in strength was observed for the B_2O_3-containing glass formulations. The tensile strength for the day-28 interval-degraded P40B5, P45B5 and P50B5 fibres was 448 ± 89, 710 ± 134 and 586 ± 47 MPa, respectively. Similar to the annealed fibres, no statistically significant change in tensile modulus was observed over the duration of the study.

Dissolution rate of the annealed and non-annealed degraded fibres

Figure 7 represents the estimated dissolution rate of annealed and non-annealed degraded fibres after 28 days of dissolution in PBS at 37°C. The estimated dissolution rate of the annealed fibres was lower than the non-annealed fibres. After 28 days of degradation, the estimated dissolution rate of non-annealed P45B0, P45B5 and P45B10 fibres was 2.53×10^{-6}, 1.97×10^{-6} and 1.47×10^{-6} g cm^{-2} h^{-1}, respectively. Whereas dissolution rate of 1.49×10^{-6}, 1.25×10^{-6} and 8.59×10^{-7} g cm^{-2} h^{-1} was observed for annealed P40B0, P45B5 and P45B10 fibres. However, for P50B0 and P50B5 fibres, the dissolution rate decreased from 8.28×10^{-6} to 2.96×10^{-6} g cm^{-2} h^{-1} and 4.50×10^{-6} to 1.35×10^{-6} g cm^{-2} h^{-1} with annealing, respectively.

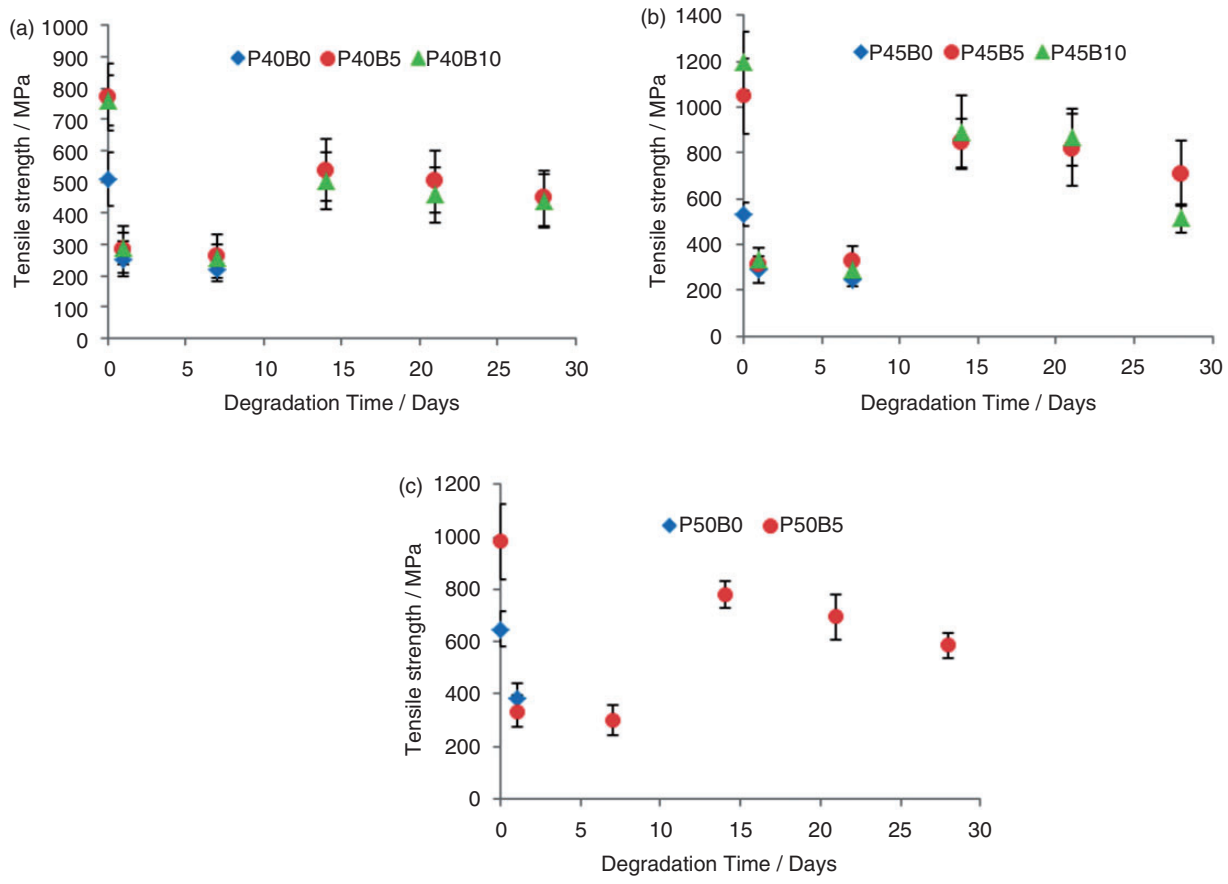

Figure 6. The change in tensile strength of the non-annealed fibres in the glass system of P40Ca16Mg24Na(20 − X)Bx (a), P45Ca16Mg24Na(15 − X)Bx (b) and P50Ca16Mg24Na(10 − X)Bx (c), where x = 0, 5 and 10 mol% during degradation in PBS at 37°C. Error bars represent the standard deviation where n = 20.

Discussion

PGFs have great potential for use in biomedical applications as the compositions of these fibres can easily be tailored to suit the end application.[28] It has been suggested that the fibre-drawing ability of PBGs strongly depends on the structure of the glass, in particular the Q speciation within the glass.[1] For example, glasses with metaphosphate structure were found to be easily converted into fibres due to the polymeric nature of these glasses as their structure was heavily dominated by Q^2 species, i.e. long-chain lengths (reportedly over 90%).[4] The degradation rates for these glasses have been reported to play a very important role on their biocompatibility.[2] Therefore, manufacture of phosphate glass fibres with the required degradation profiles for the intended application along with favourable cytocompatibility is highly desired. With this in mind, it was hypothesised that increased B_2O_3 content in the glass formulation could enhance the fibre-drawing ability of PBGs and the durability of these fibres.

Glass formulations containing 5 and 10 mol% B_2O_3 with P_2O_5 contents fixed at 40, 45 and 50 mol% were found to be considerably easier to form fibres than the non-B_2O_3-containing glasses. It was also possible to draw fibres from these formulations continuously without breakage. However, it was not possible to draw fibres from the P50B10 glass formulation (50 mol% P_2O_5 and 10 mol% B_2O_3) as the glass would not exit from the bushing tip due to the viscosity of this melt at the maximum temperature limit for the in-house melt-drawn fibre production system used. Ahmed et al.[1] investigated fibre manufacture from glass fibres fixed with 45, 50 and 55 mol% P_2O_5. They reported that it was possible to obtain fibres from the 50 and 55 mol% P_2O_5 compositions; however, fibre manufacture from glasses with fixed 45 mol% P_2O_5 proved to be unsuccessful, which was attributed to the low viscosity and short average chain length of the glass compositions. Ahmed et al.[4] reported that PBG formulations with P_2O_5 content fixed at 45 mol% were composed of shorter chains due to a mixture of Q^2 and Q^1 species (with the Q^1 and Q^2 ratios reportedly to be in the range of ~17–20 and ~78–82, respectively). Whereas formulations, where P_2O_5 content was fixed at 50–55 mol%, reportedly had a long-chain structure composed mostly

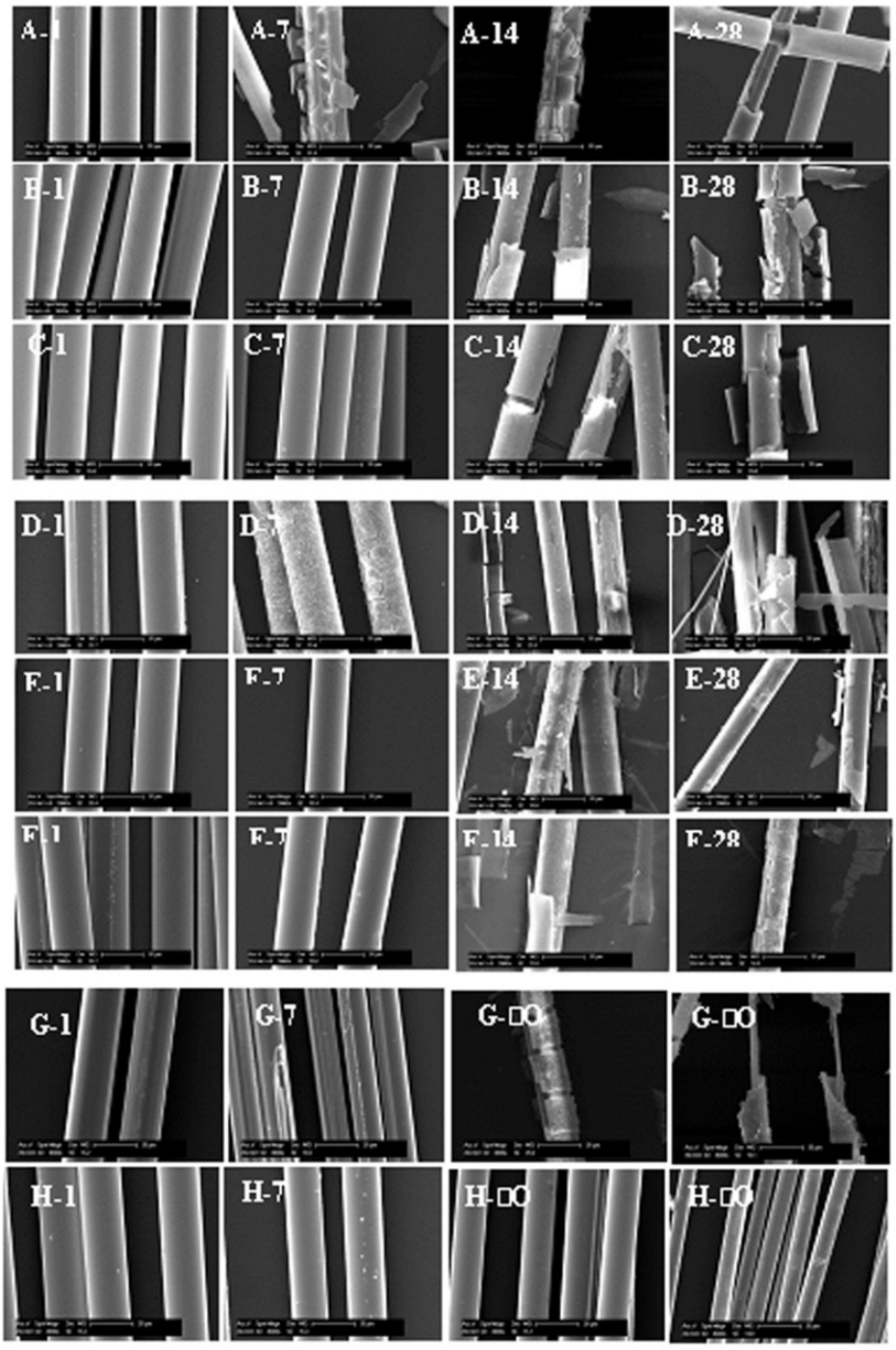

Figure 7. Scanning electron microscopy of days 1, 14 and 28 non-annealed degraded fibres of the composition P40B0 (A1–A28), P40B5 (B1–B28), P40B10 (C1–C28), P45B0 (D1–D28), P45B5 (E1–E28), P45B10 (F1–F28), P50B0 (G1–G28) and P50B5 (H1–H28). The fibres were degraded in PBS at 37°C for up to 28 days.

of Q^2 chains (Q^1 and Q^2 ratios were reported to be in the range of ~0.3–3 and ~96–99, respectively).[4]

In this study, it was found that the addition of 5 and 10 mol% B_2O_3 allowed for fibre manufacture from glass formulations with P_2O_5 content fixed at 45 mol%, and this fibre production was continuous with no breakage for up to 3 h. Furthermore, addition of B_2O_3 (5–10 mol%) also made it possible to pull continuous fibre from glass formulations fixed at an even lower phosphate content of 40 mol% P_2O_5, which hitherto had not been possible in our research group. Saranti et al.[16] suggested that the addition of boron

could alter the dimensionality of the phosphate network via the formation of long-chain Q^2 species rather than Q^0 or Q^1 units. Therefore, it is suggested that an increase in the chain length (i.e. Q^2 species) due to addition of B_2O_3 helped to ease manufacture of fibres from phosphate glass formulations with fixed P_2O_5 contents of 40 and 45 mol%.

Murgatroyd[29] stated that successful fibre drawing depended on the strength of the bonds in the glass structure and that it was possible to draw fibre from melts if the bonds were strong enough to withstand the stresses from the pulling process even at the high temperatures employed for fibre drawing. Whereas weak P-O-P bonds could be extended for a short distance along the strong bonds, but would not be able to form continuous fibres. It was also suggested that continuity of the fibre-drawing process depended on the ability of the strongest bonds to hold together as they were pulled out of the melt.[29] Thus, the ease of fibre drawing from B_2O_3-containing glass compositions provided empirical evidence that addition of B_2O_3 to the glass structure introduced stronger bonds to the glass, which in turn helped to improve their fibre-drawing characteristics.

The glass series investigated exhibited a trend of increasing fibre strength with increasing B_2O_3 and P_2O_5 content. The tensile strength was found to have increased by 42%, 50% and 52% via addition of 5 mol% B_2O_3 to P40, P45 and P50 glass formulations, respectively. Whereas an increase of 81% and 126% in the tensile strength was observed when 10 mol% B_2O_3 was added to the P40 and P45 glass systems. The highest tensile strength (1200 ± 130 MPa) was observed for P45B10 fibres, and to the best of the authors' knowledge, the highest tensile strength has ever been reported for PGFs.

Cozien-Cazuc et al.[30] reported the tensile strength of fibres drawn from the glass system $40P_2O_5$-16CaO-24MgO-$10Na_2O$ to be 484 ± 153 MPa. The values obtained by Cozien-Cazuc et al.[30] compared well with the values obtained from this study (450 ± 56 MPa) for the same formulation (quoted as P40B0). Ahmed et al.[31] studied the mechanical properties of fibres drawn from $50P_2O_5$-40CaO-$5Na_2O$-$5Fe_2O_3$ glass and reported the tensile strength and modulus to be 456 MPa and 51.5 GPa, respectively. The average tensile strength and modulus of 40 P_2O_5-24 MgO-16 CaO-$16Na_2O$-4 Fe_2O_3 fibres were reported to be 318 ± 46 MPa and 73 ± 10 GPa, respectively, by Felfel et al.[32] The tensile strengths of the fibres observed by Ahmed et al.[31] and Felfel et al.[32] were significantly lower than the values obtained in this study for B_2O_3 (5 and 10 mol%) containing fibres with P_2O_5 contents fixed at 40, 45 and 50 mol%.

It is well known that the strength of glass is affected by its average bond strength, which depends on the chemical composition of the glass.[33] The cationic field strength is also known to have a strong effect on the mechanical properties of the glass.[34] Kurkjian[34] studied the mechanical properties of phosphate glass fibres drawn from $NaPO_3$, $Zn(PO_3)_2$, 20 mol% K_2O-10 mol% MgO-10 mol% Al_2O_3-60 mol% P_2O_5 and 40 mol% Fe_2O_3-60 mol% P_2O_5 glass compositions. He reported that replacing monovalent sodium with divalent zinc or trivalent/divalent iron, the modulus and strength of the fibres increased. He suggested that this improvement in mechanical properties was due to the increased cross-linking caused by replacing the monovalent cations with the divalent or trivalent cations.

In this study, the tensile strength of the fibres was seen to significantly increase (from ~42 to 56%) as B_2O_3 (5–10 mol%) was added to the glass systems. It has been reported that the addition of B_2O_3 to the phosphate glass structure can form highly cross-linked BPO_4 units, which are composed of interconnected BO_4 and PO_4 tetrahedral units.[35,36] Thus, it is suggested that the increased cross-link density with increasing B_2O_3 content was responsible for the increased tensile strength of the fibres produced. Shah et al.[37] studied the effect of B_2O_3 addition on the structure and microhardness of glasses in the system $40Na_2O$-xB_2O_3-$(50-x)P_2O_5$. They reported that cross-linking between the phosphate chains increased with increasing amount of B_2O_3 in the glass systems. They also reported an increase in microhardness as P_2O_5 was replaced with B_2O_3 and suggested that this was due to the formation of stronger P-O-B linkages. Moreover, the inclusion of a second network former to PBGs increased the strength and elastic modulus owing to the strong interaction between chain structures and the formation of three-dimensional structures.[38] As B_2O_3 is a natural glass network former,[17,19,39] its influence could be explained either by borate ion action as a network modifier (creating ionic cross-linking as discussed above) or becoming part of the glass network (i.e. entering the backbone of the glass network). Therefore, along with cross-linking, the borate ions can also participate in the formation of chain structures, i.e. become a part of the backbone of the glass network. Therefore, the improvement in fibre strength with addition of B_2O_3 could be attributed to the fact that addition of boron to the phosphate glass network increased the cross-linking density and chain lengths by becoming or forming part of the glass network as also evidenced by higher T_g and enhanced processing window highlighted in a previous publication.[40]

The Weibull modulus of the fibres studied in the present study was seen to range from 7.7 to 10.5. Karabulut et al.[41] studied the tensile strength of a series of PGFs drawn by melt-drawn system. They found Weibull modulus values in the range of 6

and 12. The Weibull modulus (m) is a well known and accepted method to describe the physics of fibre failure.[42] If a value of m is large, then stresses even slightly below the normalising value σ_o would lead to a low probability of failure. However, a low-Weibull modulus would introduce uncertainty about the strength of the fibre.[27]

The tensile modulus of the fibres was found to increase with increasing B_2O_3 content. The tensile modulus of a material is an intrinsic property and depends on the field strength of the cation and the packing density of the oxygen atoms.[43] Like tensile strength, the tensile modulus also increases with increasing cationic field strength.[38] Pukh et al.[38] reported that for inorganic glasses, addition of cations with higher field strength interacts strongly with the negatively charged phosphate anions and therefore hinders the mutual rotations and displacements of the anions. This interaction increased with increasing cationic charge, which eventually increased the tensile modulus.

Annealed fibres showed a significant increase ($P < 0.01$) in tensile modulus, whilst the tensile strength decreased upon annealing. Murgatroyd[44,45] had previously studied the effect of heat treatment on the elastic properties of silica-based fibres and reported that heat treatment increased the Young's modulus. The author suggested that a profound change in the glass constitution took place during the fibre-drawing process. The extension process during the fibre drawing caused long chains of molecules to be formed in the direction of the pull, whilst a larger number of lateral bonds in the glass melt were broken. The author proposed that during the heat-treatment process, the long chains might break up and become displaced in the axial direction, which would lead to the increased Young's modulus values. Murgatroyd[44,45] also suggested that the lateral bonds formed during heat treatment coincided with a loss of ductility, which eventually decreased the tensile strength of the fibres.

A strong structural anisotropy due to the alignment of the phosphate chains along the main axis of the PGFs has been reported in several studies, and this structural anisotropy has been correlated with the fibre-drawing process.[46,47] Stockhorst and Brunker[46] reported that annealing enabled relaxation of the phosphate chains from the oriented structure to a disordered entangled structure, which was quite similar to that of the corresponding bulk glass. Thus, the loss of anisotropy and structure orientation of the fibres during annealing were suggested to be responsible for the reduction in their tensile strength.

Heat treatment (annealing) can also reduce the internal stresses of the fibres, which are introduced due to the rapid cooling of the fibres during their manufacturing process. Otto[8] suggested that during annealing, the structure rearranged itself to attain a more stable configuration by reforming broken bonds and allowing some bonds to reach a more stable state, and the structures became more compact or dense. Begum et al.[48] suggested that heat treatment resulted in the reduction in interatomic spaces, which could contribute to an increase in density. For comparison, the density of the annealed and non-annealed fibres was measured, and it was found that the density of the annealed fibres was significantly higher than the non-annealed ones. Thus, it was confirmed that annealing introduced a denser structure to the fibres due to the atomic rearrangement, which led to an increase in modulus as seen in Figure 7.

The trend for the dissolution properties of annealed B_2O_3-containing fibres suggested that the tensile strength of the degraded fibres increased up to day 45 and then decreased by day 60. Whilst, for the non-annealed B_2O_3-containing fibres, the initial mechanical properties rapidly decreased to half their initial value by day 7 and then increased by day 14. With further degradation, a slow reduction in the tensile strength was observed with time.

Cozien-Cazuc et al.[30] also observed an increase in strength of degraded annealed P40 Ca16 Na20 Mg24 fibres and suggested that the improved tensile strength was due to the removal of the outer tensile layer. The cracking or peeling effect of the outer-hydrated layer of the annealed fibres was also observed by Choueka et al.[49] Choueka et al.[50] compared the mass loss and surface morphology of annealed and non-annealed phosphate-based fibres. They reported that the degradation rate of the annealed fibres was 50% less than the non-annealed ones, and the annealed fibres maintained their structural integrity for a longer period of time. They also suggested that rapid cooling in combination with the pulling process during fibre production placed inherent stresses in the fibres. Annealing thus minimised the effect of stress and reformed the bonds allowing some of them to rotate into more stable configurations. These annealed fibres may have decreased mechanical properties, but will have an increased chemical durability, which allowed it to retain its original strength for a longer period of time.[50] Due to this stable structure, the annealed fibres were more durable than the non-annealed ones.

The surface morphology of the annealed degraded fibres remained smooth up to day 14 of degradation. The peeling effect of the outer layer of annealed degraded fibres was observed from day 21. As compared with the tensile strength of day 1-degraded fibres, a significant improvement ($P < 0.01$) in tensile strength for degraded fibres was also observed from day 21. From the SEM images, it was clear that the

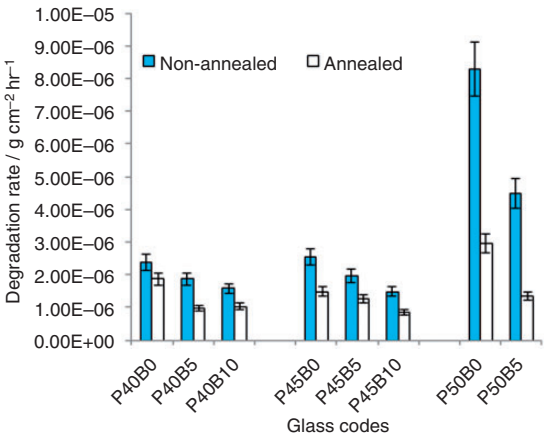

Figure 8. Degradation rate of annealed and non-annealed fibres in the glass system of P40Ca16Mg24Na(20 − X)Bx, P45Ca16Mg24Na(15 − X)Bx and P50Ca16Mg24Na(10 − X)Bx, where x = 0, 5 and 10 mol% during degradation in PBS at 37°C.

change in surface morphology during degradation of the non-annealed fibres was similar to those found for the annealed fibres. However, the degradation rate of the non-annealed fibres was much faster than the annealed ones as the peeling effect of the outer layer for non-annealed fibres was observed from day 7 as compared to day 21 for the annealed fibres. It could also be seen that the reduction in diameter of the non-annealed fibres was much faster than for the annealed ones.

For comparison, the dissolution rate of the annealed and non-annealed fibres was calculated using diameter and density of the degraded fibres at different time points for P45B0, P45B5 and P45B10 formulations (Figure 8). It was found that the dissolution rate of the annealed degraded P45B0, P45B5 and P45B10 fibres was 42%, 38% and 47% lower than the non-annealed ones. Moreover, it was still possible to handle and test the annealed fibres for a longer period of time as compared to the non-annealed ones. Cozien-Cazuc et al.[30] found that after 24 h of degradation, the dissolution rate of non-annealed fibres was 2×10^{-7} g cm^{-2} min^{-1}, whereas the annealed fibres showed a much lower degradation rate, i.e. 1.1×10^{-7} g cm^{-2} min^{-1}. Hayden et al.[51] suggested that a surface tensile stress layer was generated in the phosphate glasses during thermal annealing due to the surface re-arrangement caused by the water vapour attack. This tensile layer could account for the initial low-tensile strength values as this layer would be prone to cracking followed by a uniform degradation.[51] Thus, an increase in tensile strength for fibres during the degradation process may be explained by the progressive removal of the outer tensile layer resulting in a reduction in the fibre diameter. Parsons et al.[42] also suggested that stress developed in phosphate glass fibres during the fibre-drawing process could be relieved by heat treatment, which would change the mode of degradation. Thus, although the initial strength of the annealed fibres was significantly lower than the as drawn fibres, annealing appeared to impart significant improvements in the durability of the fibres. A decrease in dissolution rate was also observed with increasing B_2O_3 content from 0 to 10 mol%. A similar decreasing trend of dissolution rate with increasing B_2O_3 content was observed for bulk glasses in a previous study.[40] This decrease in dissolution rate with increasing B_2O_3 was attributed to the replacement of P-O-P bonds with P-O-B bonds, which also correlated well with an increase in T_g and a decrease in thermal expansion coefficient.

No significant change in the tensile modulus of the fibres was observed during degradation, which correlated with the results found by Cozien-Cazuc et al.[30] They carried out degradation of phosphate glass fibres in doubly distilled water at 37°C for 3 days and found that there was no significant change in fibre modulus during this period. They suggested that degradation took place from the surface of the fibres, and no intrinsic change in glass structure was caused by their dissolution.[30]

In summary, this study showed that incorporation of B_2O_3 had a significant effect on the fibre-drawing process and also on the mechanical properties of the fibres. This ease of fibre formation and higher mechanical properties was attributed to the extension of phosphate chain length and increased cross-linking. These PBG fibres have great potential as reinforcement for bioresorbable composites, which are currently under investigation.

Conclusions

Nine PBG compositions in the system P_2O_5-CaO-Na_2O-MgO-B_2O_3 were produced by replacing the Na_2O with B_2O_3, and the P_2O_5 content was varied at 40, 45 and 50 mol%. Addition of B_2O_3 to the glass system enabled successful drawing of continuous fibres from glasses with phosphate (P_2O_5) contents of 40, 45 and 50 mol%. It was also possible to draw fibres from all the compositions with exception of P50B10 due to high viscosity of the melt at the maximum temperature limit for the in-house melt-draw system used. The mechanical properties of the fibres increased with increasing B_2O_3. P45B10 fibres provided the highest tensile strength (1200 ± 146 MPa), which is the highest reported strength to date for <25-μm phosphate glasses fibres suited for composite reinforcement. Comparison of mechanical properties of the annealed and non-annealed fibres revealed that with annealing, the tensile

strength decreased whilst the tensile modulus increased. In addition, the degradation rate of the annealed fibres was much slower as compared to the non-annealed ones. Both annealed and non-annealed fibres exhibited a peeling effect of the fibre's outer layer during degradation. The strength of the fibres was found to increase with degradation, and it was postulated that the increase was due to the removal of the outer tensile layer during the period of degradation.

References

1. Ahmed I, Lewis M, Olsen I, et al. Phosphate glasses for tissue engineering, Part 2: processing and characterisation of a ternary-based P_2O_5–CaO–Na_2O glass fibre system. *Biomaterials* 2004; 25: 501–507.
2. Knowles JC. Phosphate based glasses for biomedical applications. *J Mater Chem* 2003; 13: 2395–2401.
3. Neel EAA, Pickup DM, Valappil SP, et al. Bioactive functional materials: a perspective on phosphate-based glasses. *J Mater Chem* 2009; 19: 690–701.
4. Ahmed I, Lewis M, Olsen I, et al. Phosphate glasses for tissue engineering, Part 1: processing and characterisation of a ternary-based P_2O_5–CaO–Na_2O glass system. *Biomaterials* 2004; 25: 491–499.
5. Brow RK. Review: the structure of simple phosphate glasses. *J Non-Cryst Solids* 2000; 263–264: 1–28.
6. Bitar M, Salih V, Mudera V, et al. Soluble phosphate glasses: in vitro studies using human cells of hard and soft tissue origin. *Biomaterials* 2004; 25: 2283–2292.
7. Ahmed IC, Lewis CA, Olsen MP, et al. Processing, characterisation and biocompatibility of iron-phosphate glass fibres for tissue engineering. *Biomaterials* 2004; 25: 3223–3232.
8. Otto WH. Compaction effects in glass fibers. *J Am Ceram Soc* 1961; 44: 68–72.
9. Felfel RM, Ahmed I, Parsons AJ, et al. Investigation of crystallinity, molecular weight change, and mechanical properties of PLA/PBG bioresorbable composites as bone fracture fixation plates. *J Biomater Appl* 2012; 26: 765–789.
10. Parsons AJ, Ahmed I, Haque P, et al. Phosphate glass fibre composites for bone repair. *J Bionic Eng* 2009; 6: 318–323.
11. Ahmed I, Parsons AJ, Palmer G, et al. Weight loss, ion release and initial mechanical properties of a binary calcium phosphate glass fibre/PCL composite. *Acta Biomater* 2008; 4: 1307–1314.
12. Han N, Ahmed I, Parsons AJ, et al. Influence of screw holes and gamma sterilization on properties of phosphate glass fiber-reinforced composite bone plates. *J Biomater Appl* 2013; 27: 990–1002.
13. Ahmed I, Jones IA, Parsons AJ, et al. Composites for bone repair: phosphate glass fibre reinforced PLA with varying fibre architecture. *J Mater Sci Mater Med* 2011; 22: 1825–1834.
14. Navarro M, Ginebra M-P, Clément J, et al. Physicochemical degradation of titania-stabilized soluble phosphate glasses for medical applications. *J Am Ceram Soc* 2003; 86: 1345–1352.
15. Brow RK and Tallant DR. Structural design of sealing glasses. *J Non-Cryst Solids* 1997; 222: 396–406.
16. Saranti A, Koutselas I and Karakassides MA. Bioactive glasses in the system CaO–B_2O_3–P_2O_5: preparation, structural study and in vitro evaluation. *J Non-Cryst Solids* 2006; 352: 390–398.
17. Qiu D, Guerry P, Ahmed I, et al. A high-energy X-ray diffraction, ^{31}P and ^{11}B solid-state NMR study of the structure of aged sodium borophosphate glasses. *Mater Chem Phys* 2008; 111: 455–462.
18. Lee ETY and Taylor ERM. Compositional effects on the optical and thermal properties of sodium borophosphate glasses. *J Phys Chem Solids* 2005; 66: 47–51.
19. Carta D, Qiu D, Guerry P, et al. The effect of composition on the structure of sodium borophosphate glasses. *J Non-Cryst Solids* 2008; 354: 3671–3677.
20. Karabulut M, Yuce B, Bozdogan O, et al. Effect of boron addition on the structure and properties of iron phosphate glasses. *J Non-Cryst Solids* 2011; 357: 1455–1462.
21. Massera J, Claireaux C, Lehtonen T, et al. Control of the thermal properties of slow bioresorbable glasses by boron addition. *J Non-Cryst Solids* 2011; 357: 3623–3630.
22. Harada T, In H, Takebe H, et al. Effect of B_2O_3 addition on the thermal stability of barium phosphate glasses for optical fiber devices. *J Am Ceram Soc* 2004; 87: 408–411.
23. Koudelka L and Mošner P. Study of the structure and properties of Pb–Zn borophosphate glasses. *J Non-Cryst Solids* 2001; 293–295: 635–641.
24. Bingham PA, Hand RJ and Forder SD. Doping of iron phosphate glasses with Al_2O_3, SiO_2 or B_2O_3 for improved thermal stability. *Mater Res Bull* 2006; 41: 1622–1630.
25. Arstila H, Vedel E, Hupa L, et al. Factors affecting crystallization of bioactive glasses. *J Eur Ceram Soc* 2007; 27: 1543–1546.
26. Ahmed I, Parsons AJ, Palmer G, et al. Weight loss, ion release and initial mechanical properties of a binary calcium phosphate glass fiber/PCL composite. *Acta Biomater* 2008; 4: 1307–1314.
27. Hull D and Clyne TW. *An introduction to composite materials*. NY: Cambridge University Press, 1996.
28. Neel EAA, Young AM, Nazhat SN, et al. A facile synthesis route to prepare microtubes from phosphate glass fibres. *Adv Mater* 2007; 19: 2856–2862.
29. Murgatroyd JB. The delayed elastic effect in glass fibres and the constitution of glass in fibre form. *J Soc Glass Technol* 1948; 32: 291–300.
30. Cozien-Cazuc SP, Walker A, Jones G, et al. Effects of aqueous aging on the mechanical properties of $P_{40}Na_{20}Ca_{16}Mg_{24}$ phosphate glass fibres. *J Mater Sci* 2008; 43: 4834–4839.
31. Ahmed IC, Neel PSA, Parsons EA, et al. Retention of mechanical properties and cytocompatibility of a phosphate-based glass fiber/polylactic acid composite. *J Biomed Mater Res, Part B: Appl Biomater* 2009; 89: 18–27.
32. Felfel RM, Ahmed I, Parsons AJ, et al. Investigation of crystallinity, molecular weight change, and mechanical properties of PLA/PBG bioresorbable composites as

bone fracture fixation plates. *J Biomater Appl* 2012; 26: 765–789.
33. Nishikubo SY, Sugawara T and Matsuoka J. Intrinsic strength of sodium borosilicate glass fibers by using a two-point bending technique. *Mater Sci Eng* 2011; 18: 112019–1-112019-4.
34. Kurkjian CR. Mechanical properties of phosphate glasses. *J Non-Cryst Solids* 2000; 263–264: 207–212.
35. Kim N-J, Im S-H, Kim D-H, et al. Structure and properties of borophosphate glasses. *Electron Mater Lett* 2010; 6: 103–106.
36. Koudelka L and Mošner P. Borophosphate glasses of the $ZnO–B_2O_3–P_2O_5$ system. *Mater Lett* 2000; 42: 194–199.
37. Shah K, Goswami M, Deo M, et al. Effect of B_2O_3 addition on microhardness and structural features of $40Na_2O$-10BaO-xB_2O_3-(50-x)P_2O_5; glass system. *Bull Mater Sci* 2006; 29: 43–48.
38. Pukh VP, Baikova LG, Kireenko MF, et al. Atomic structure and strength of inorganic glasses. *Phys Solid State* 2005; 47: 876–881.
39. Rinke MT and Eckert H. The mixed network former effect in glasses: solid state NMR and XPS structural studies of the glass system $(Na_2O)x(BPO_4)1$-x. *Phys Chem Chem Phys* 2011; 13: 6552–6565.
40. Sharmin N, Hasan MS, Parsons AJ, et al. Effect of boron addition on the thermal, degradation, and cytocompatibility properties of phosphate-based glasses. *BioMed Res Int* 2013; 2013: 12.
41. Karabulut M, Melnik E, Stefan R, et al. Mechanical and structural properties of phosphate glasses. *J Non-Cryst Solids* 2001; 288: 8–17.
42. Parsons AJ, Ahmed I, Yang J, et al. Heat-treatment of phosphate glass fibres and its effect on composite property retention. In: *16th international conference on composite materials*. Kyoto, 2007.
43. Baikova LG, Fedorov YK, Tolstoi MN, et al. Structural strength of phosphate glasses. *Sov J Glass Phys Chem* 1991; 16: 211–217.
44. Murgatroyd JB. The strength of glass fibres, Part 1: elastic properties. *J Soc Glass Technol* 1944; 28: 368–387.
45. Murgatroyd JB. The delayed elastic effect in glass fibres and the constitution of glass in fibre form. *J Soc Glass Technol* 1948; 32: 291–300.
46. Stockhorst HB and Brunker R. Structure sensitive measurements on phosphate glass fibers. *J Non-Cryst Solids* 1986; 85: 105–126.
47. Muñoz F, Pritula O, Sedlá J, et al. A study on the anisotropy of phosphate glass fibres. *Glass Technol—Eur J Glass Sci Technol Part A* 2008; 49: 47–52.
48. Begum AN, Rajendran V and Ylänen H. Effect of thermal treatment on physical properties of bioactive glass. *Mater Chem Phys* 2006; 96(2–3): 409–417.
49. Choueka J, Charvet JL, Alexander H, et al. Effect of annealing temperature on the degradation of reinforcing fibers for absorbable implants. *J Biomed Mater Res* 1995; 29: 1309–1315.
50. Choueka J, Charvet JL, Alexander H, et al. Effect of annealing temperature on the degradation of reinforcing fibers for absorbable implants. *J Biomed Mater Res* 1995; 29: 1309–1315.
51. Hayden JS, Iii AJM, Suratwala TI, et al. Surface tensile layer generation during thermal annealing of phosphate glass. *J Non-Cryst Solids* 2000; 263–264: 228–239.